Hysteresis losses in MgB_2 superconductors exposed to combinations of low AC and high DC magnetic fields and transport currents

N. Magnusson[a,*], A.B. Abrahamsen[b], D. Liu[c], M. Runde[a] and H. Pollinder[c]

[a]SINTEF Energy Research, NO-7465 Trondheim, Norway
[b]DTU Wind Energy, Technical University of Denmark, DK-4000 Roskilde, Denmark
[c]Electrical power processing group, TU Delft, Mekelweg 4, NL-2628 CD Delft, Netherlands

[*]Corresponding author: Tel. +47 90718577; e-mail: niklas.magnusson@sintef.no

Abstract
MgB_2 superconductors are considered for generator field coils for direct drive wind turbine generators. In such coils, the losses generated by AC magnetic fields may generate excessive local heating and add to the thermal load, which must be removed by the cooling system. These losses must be evaluated in the design of the generator to ensure a sufficient overall efficiency. A major loss component is the hysteresis losses in the superconductor itself. In the high DC – low AC current and magnetic field region experimental results still lack for MgB_2 conductors. In this article we reason towards a simplified theoretical treatment of the hysteresis losses based on available models in the literature with the aim of setting the basis for estimation of the allowable magnetic fields and current ripples in superconducting generator coils intended for large wind turbine direct drive generators. The resulting equations use the DC in-field critical current, the geometry of the superconductor and the magnitude of the AC magnetic field component as parameters. This simplified approach can be valuable in the design of MgB_2 DC coils in the 1 - 4 T range with low AC magnetic field and current ripples.

Key words: Generator field winding, ac losses, magnesiumdiboride

1 Introduction

MgB_2 superconductors are, for their low cost compared to the high-temperature YBCO conductors, and higher operating temperature than the low-temperature Nb_3Sn and NbTi superconductors, considered for several DC applications in the medium magnetic flux density range of 1 - 4 T. These applications include e.g. MRI magnets [1] and [2], magnets for induction heaters [3], and the field windings of wind power generators [4] and [5]. Under pure DC conditions the MgB_2 coils are practically loss-free (except for joints). However, the presence of a time-varying magnetic field inevitably results in energy losses. Although these losses generally are small, they add to the total heat load to be handled by the cryogenic system, and maybe more important, they result in local heating of the coil. Therefore, the coil needs to be thermally designed to withdraw the heat caused by the AC losses, or expressed alternatively; the losses need to be suppressed to a value not jeopardizing the operation of the coil.

In the design of MgB_2 superconducting generator field coils for direct drive wind turbine generators, the overall loss of the drive train must be kept within or below the range of 5-10% of the transferred power to be feasible, and local excessive heating must be prevented. Superconducting field coils may be applied to synchronous generators, where the armature is made of conventional copper conductors at ambient temperature. Thus, under normal operating conditions, the superconductor is primarily exposed to the coil's self-field and the magnetic field created by the armature. These two magnetic fields are superpositioned and include AC ripples (from the armature harmonics and from the excitation circuit of the field coil).

Here we focus on the hysteresis losses appearing under normal operation, i.e. the superconductor is exposed to a relatively low AC magnetic field superimposed on a bias DC field, as well as a low AC current superimposed on a bias DC current. Hence, flux-creep and flux-flow losses related to the instantaneous level of the current relative the critical current, which are of less importance if the coil is operated with a sufficient margin to the critical current, are not considered. Neither are eddy currents, losses during ramping of the coils and losses due to electrical faults.

Some experimental work has been done on AC losses of MgB_2, see e.g. [6], [7], [8] and [9], but measurements of AC losses due to an AC ripple on a DC magnetic field in the 1-4 T range still lack. Although results from calculations for an NbTi wind power generator design are given in [10], there is a need to establish methods for calculation of the losses in the design phase of MgB_2 based

generators. The mechanism leading to AC losses in multi-filamentary superconductors is quite complicated, and there exists a wide variety of different loss equations and modelling tools covering different geometries and load cases. In this article we reason towards the use of a limited number of existing loss equations based on the critical state model to estimate the hysteresis losses for an MgB_2 coil with AC field and current components that are small compared to the DC components, as is the case in the field windings of generators for wind turbines.

2 Hysteresis loss models

2.1 Critical state model

Hysteresis losses in superconductors are commonly discussed in the framework of the critical state model [11] and [12] considering the vortex dynamics inside the superconductor. In the model, the magnetic flux density, $\boldsymbol{B}$, follows

$$|\boldsymbol{\nabla}\times\boldsymbol{B}| = \mu_0 J_{\boldsymbol{c}} \,, \tag{1}$$

where J_c is the critical current density. When an external magnetic field is increased, vortices enter into the superconductor from its surfaces. However, the vortices are hindered to move until J_c is reached (then the Lorentz-like force on the vortices equals the pinning force). As J_c is reached the vortices can move further into the superconductor, and they build up a flux distribution according to (1). Hence, the current density inside the superconductor has to be either J_c or zero (thereby the name critical state model). When the external magnetic field then is reduced, the vortices exit the superconductor from its surfaces, creating an irreversible magnetic flux pattern and leading to hysteresis losses.

2.2 Basic analytic loss equations for AC magnetic fields

Based on the critical state model, several loss equations and calculation methods have been developed. A simple case is an AC magnetic field in parallel with a slab, infinite in two directions and with a width a in the third. Introducing the field of full penetration, B_p (the field at which the vortices reach the centre of the superconducting slab),

$$B_p = \frac{\mu_0 J_c a}{2} \,, \tag{2}$$

the hysteresis losses per unit length, P_l, can be expressed by [12],

$$P_l = \begin{cases} \dfrac{2fA}{3\mu_0 B_p} B_{ac}^3 & for \quad B_{ac} \le B_p \\ \dfrac{2fAB_p}{3\mu_0}\left(3B_{ac} - 2B_p\right) & for \quad B_{ac} \ge B_p \end{cases} , \tag{3}$$

where f is the frequency, A the conductor area (considering a finite conductor approximated with the slab geometry), and B_{ac} the peak applied AC magnetic field. As can be seen, for low magnetic fields P_l is proportional to B_{ac}^3 for low applied fields and to B_{ac} for high applied fields. This field behaviour is typical for most wire geometries (with the exception for the strip geometry in perpendicular field [13]), although the factors in front vary with geometry.

Equation (3) has been extended to include transport currents both below [14] and above [15] the critical current, I_c.

2.3 Approach for the low AC – high DC magnetic field limit

Equation (3) has also been extended to include both AC and DC components of applied magnetic fields and transport currents [16]. Different loss equations are applied for different relationships between the AC and DC components. For convenience we introduce $b_{ac} = B_{ac}/B_p$, $i_{ac} = I_{ac}/I_c$ and $i_{dc} = I_{dc}/I_c$, where I_{ac} is the peak of the applied AC transport current and I_{dc} is the applied DC transport current. Furthermore, we are interested in small ripples corresponding to the cases where b_{ac} and i_{ac} are small compared to 1-i_{dc}, i.e. smaller than the operating margin to the critical current. We are then left with two load cases for the hysteresis losses [14],

$$P_l = \begin{cases} \dfrac{2fAB_p^2}{3\mu_0}\left(b_{ac}^3 + 3b_{ac}i_{ac}^2\right) & for \quad i_{ac} \le b_{ac} \le 1 - i_{dc} \\ \dfrac{2fAB_p^2}{3\mu_0}\left(i_{ac}^3 + 3i_{ac}b_{ac}^2\right) & for \quad b_{ac} \le i_{ac} \le 1 - i_{dc} \end{cases} . \qquad (4)$$

In these two load cases (unlike all other load cases) the losses are independent of the DC component of the current, and (like all cases) independent of the DC component of the magnetic field. However, the DC component of the magnetic field influences both I_c and B_p which will be considered later in the article.

To simplify the expressions further, we consider the operating conditions of a wind turbine generator MgB_2 coil. In the crucial high-field region (the inner part) of the coil, the DC magnetic field is of the order 3 - 4 T, much higher than B_p (which typically is a factor 10 or more, lower), and therefore b_{ac} is much larger than i_{ac}, and only the upper part of (4) needs to be considered. Furthermore, the second term within the parenthesis becomes small compared to the first in the interesting region of the coil and hence, one may estimate the losses accurately (or accurately enough) by only considering the magnetic field's AC component (and not the current's AC component). Interestingly, the equation remaining is identical to the upper part of (3) yielding a convenient treatment of the losses due to small ripples in high field coils.

The weak dependence of a DC current (significantly lower than the critical current) on the AC losses due to a low AC current ripple has been shown experimentally in e.g. [16] and [17], and the weak dependence of a DC magnetic field on low magnetic field ripple in e.g. [18] and [19], all those for multifilamentary BSCCO/Ag tapes, expected to behave quantitatively similar to MgB_2 wires with respect to AC losses.

2.4 Handling the wire geometry and magnetic field orientation

The quantitative behaviour above was deduced for slab geometry and with a magnetic field in parallel with the slab. The losses are however, largely dependent on the geometry and field orientation. For tape-shaped superconductors the losses due to magnetic fields perpendicular to the face of the tape are often an order of magnitude larger than the losses due to parallel or longitudinal fields [20]. Models for how to treat the different field orientations based on weighing the losses from the parallel and perpendicular fields are presented in [21], [22] and [23]. However, calculating the

losses from the two magnetic field components separately generally gives sufficiently accurate results. In the middle of the coil the parallel magnetic field component dominates, whereas at the coil ends the perpendicular field component dominates. Only in a small part of the coil (and not where the losses are highest) are the components of comparable magnitude. Thus, we combine the total losses P_{total} according to,

$$P_{total} = P_{para} + P_{perp} \ , \tag{5}$$

where P_{para} is the loss due to the parallel field component and P_{perp} is the loss due to the perpendicular field component.

To account for the shape of the superconductor we use a model for elliptical cross-sections and arbitrary aspect ratios developed by ten Haken et al. [24] and based on the critical state model. An elliptical cross-section (including circular as a special case) describes well how the superconducting filaments are arranged in many MgB_2 conductors, and the model accounts for both losses due to parallel and perpendicular magnetic fields (by setting the aspect ratio, α, above or below unity, see Fig. 1). The model can be expressed by the following set of equations (following the notation in [24]):

$$P_l = fAM_pB_p(\alpha)q(b) \ , \tag{6}$$

$$M_p = \tfrac{2}{3\pi} J_c d \quad , \tag{7}$$

$$B_p(\alpha) = \begin{cases} \dfrac{\mu_0 J_c d}{\pi} \dfrac{\alpha}{\sqrt{\alpha^2-1}} \arctan\sqrt{\alpha^2-1} & for \quad \alpha \geq 1 \\ \dfrac{\mu_0 J_c d}{\pi} \dfrac{\alpha}{2\sqrt{1-\alpha^2}} \ln\left(\dfrac{1+\sqrt{1-\alpha^2}}{1-\sqrt{1-\alpha^2}}\right) & for \quad \alpha < 1 \end{cases} \ , \tag{8}$$

$$q(b) = \begin{cases} 4\left[\dfrac{2}{1-m'_0}\left((1-b)^{1-m'_0}-1\right)+b\left((1-b)^{-m'_0}+1\right)\right] & for \quad b < 1 \\ 4\left[b-\dfrac{2}{1-m'_0}\right] & for \quad b \geq 1 \end{cases} \ , \tag{9}$$

$$b = \frac{B_{ac}}{B_p(\propto)} \quad , \tag{10}$$

$$m'_0(\alpha) = \begin{cases} -\dfrac{3}{2}\dfrac{\alpha+1}{\sqrt{\alpha^2-1}} \arctan\sqrt{\alpha^2-1} & for \quad \alpha \geq 1 \\ -\dfrac{3}{2} \dfrac{\alpha+1}{2\sqrt{1-\alpha^2}} \ln\left(\dfrac{1+\sqrt{1-\alpha^2}}{1-\sqrt{1-\alpha^2}}\right) & for \quad \alpha < 1 \end{cases} \ , \tag{11}$$

where d is the width of the ellipse according to Fig. 1. It is notable that B_p in (8) becomes equal to (2) for large aspect ratios and, for $\alpha = 1$ both B_p and the losses attain the values derived for a round wire [25].

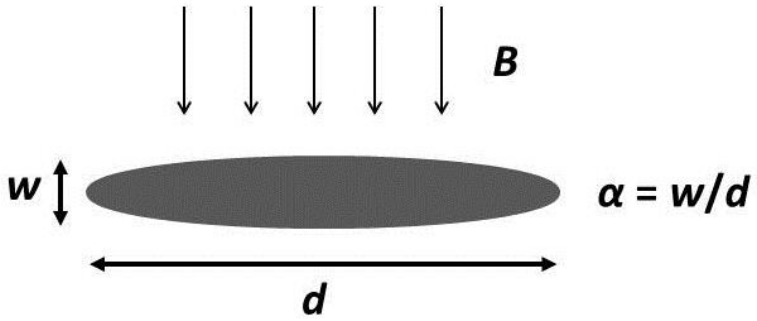

Fig. 1: Definition of *d*, *w* and *α* for a superconductor with an elliptical cross-section.

The model fits fairly well with results in the literature, e.g. [20] and [24] for BSCCO/Ag tapes and [26] for a round and a rectangular MgB_2 conductor using the dimensions of the cross-section of the elliptic filament region (not the entire conductor).

2.5 Approach to estimate the ripple losses in an MgB_2 coil for wind turbine generators

Following the reasoning in Sections 2.1 - 2.4, we propose first to use (6) - (11) to estimate the losses due to parallel and perpendicular fields separately, and secondly to add them according to (5). Equations (6) - (11) assume a field independent critical current density. In a large coil, J_c varies with the position in the coil, due to the strongly varying DC magnetic field and possibly also temperature, but varies only insignificantly with the ripple field. Consequently, $J_c(B_{dc},T)$ should be used in (7) and (8), where B_{dc} is the DC magnetic field and T the temperature. For the purpose of roughly estimating the losses we propose to use a uniform current distribution in the conductors in a FEM calculation to determine the local magnetic field, although a more rigorous approach [27] may give a somewhat more accurate field distribution. Finally, to calculate the total losses of a coil, (5) - (11) are integrated over the entire coil volume.

3 Modelled results

3.1 Wire and load case

To illustrate the dependence of the losses on ripple amplitude and DC level of the magnetic field, we chose the conductor from [5], manufactured by Columbus Superconductors. The cross-section of the superconductor is 0.5 mm x 3 mm, and the area containing the 19 superconducting filaments is assumed approximately elliptic with d = 2.6 mm and α = 0.13. The conductor is non-twisted. The $I_c(B)$ curve is given in Fig. 2 for 16 K, which is chosen as the operating temperature. In the higher end of the field range some anisotropy appears, but for simplicity we assume an isotropic $I_c(B)$ in the following. Depending on the generator design, the ripple may be of different frequencies. Therefore, we start discussing the losses in terms of loss per cycle and meter, $Q_l = P_l/f$. The operating DC current is set to 100 A.

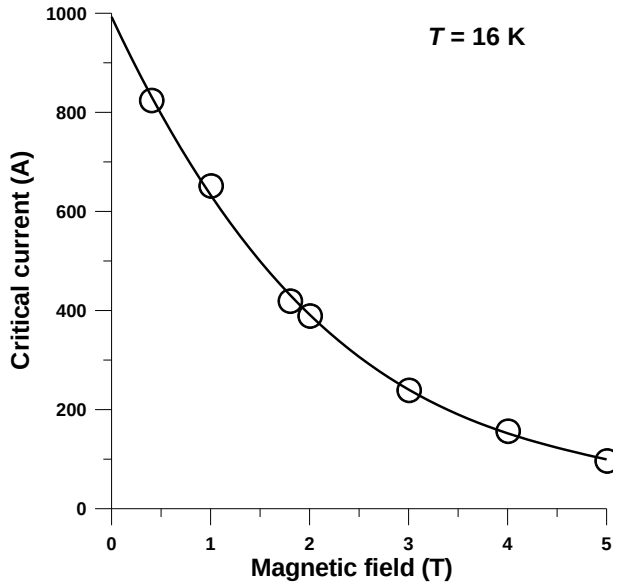

Fig. 2: Critical current as function of magnetic field (applied perpendicular to the face of the conductor) at 16 K. The rings represent measured values [5], and the line is fitted to the data and used in the modelling below.

3.2 Losses for different fields

In Fig. 3 the losses per cycle at 16 K are given as function of AC magnetic field ripple (parallel and perpendicular to the wide side of the conductor) for different DC magnetic fields. The different levels of DC magnetic field represent different positions in a coil. The losses at B_{dc} = 4 T and parallel AC ripple are only modelled up to 30 mT, where $b_{ac} \approx 1 - i_{dc}$, which is the limiting value for the model according to (4). For perpendicular field ripple, B_p is higher and thus b_{ac} lower compared to B_p and b_{ac} in parallel direction.

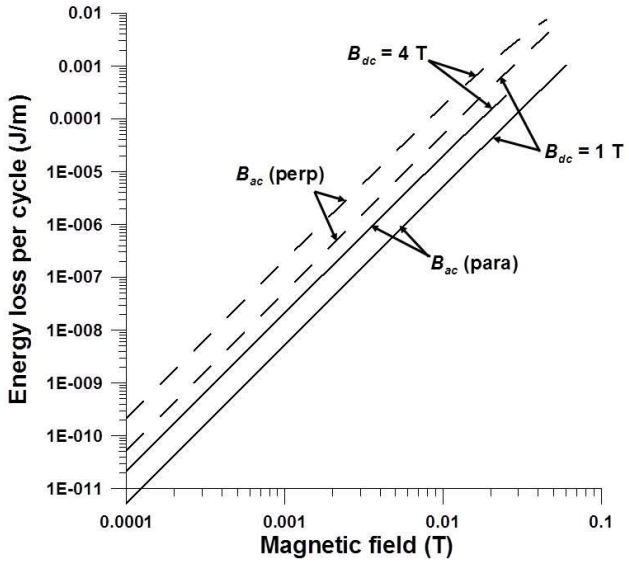

Fig. 3: Modelled losses per cycle and meter as function of AC magnetic field ripple directed parallel (solid lines) and perpendicular (dashed lines) to the wide side of the conductor at 1 T and 4 T DC magnetic fields.

In this low AC field region, the losses are proportional to the cube of the ripple field, and hence, a small increase in ripple magnitude results in a large increase in losses. Or vice versa, the losses can be greatly reduced by a moderate reduction in ripple field. Fig. 3 also shows that for this particular conductor, the losses at perpendicular fields are a factor of 10 higher than those due to parallel fields.

The dependence on the field orientation is shown in Fig. 4. From the loss value at 0° (parallel field), the losses increase at field angles above 10° as the perpendicular field starts to contribute and after approximately 30° dominates the losses.

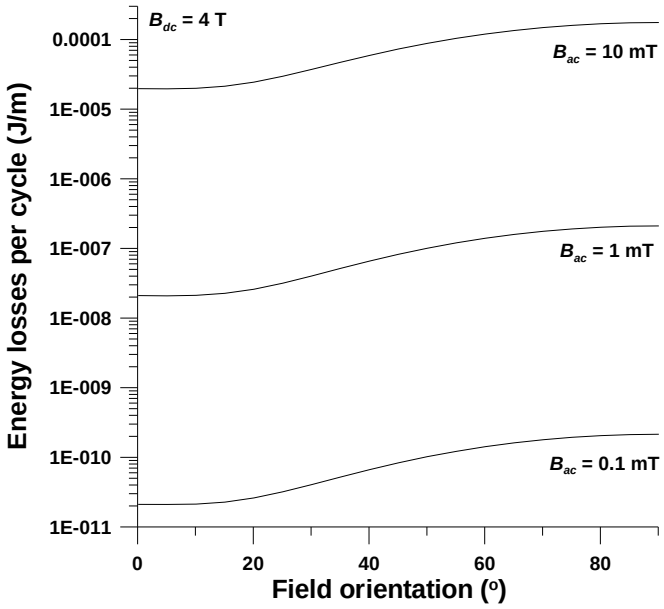

Fig. 4: Modelled losses per cycle as function of the orientation of the AC ripple field. The AC magnetic field ripple is parallel at 0° and perpendicular at 90° to the wide side of the conductor. The background DC field is 4 T.

The losses above have been presented in the form of losses per cycle. The hysteresis losses are proportional to the frequency as presented in Fig. 5 for three different magnitudes of the ripple magnetic field at a background DC field of 4 T. Different ripple frequencies may occur in a generator coil, and as can be seen in Fig. 5, a ripple of 0.1 mT at 1000 Hz equals a ripple of 1 mT at 1 Hz in terms of loss level.

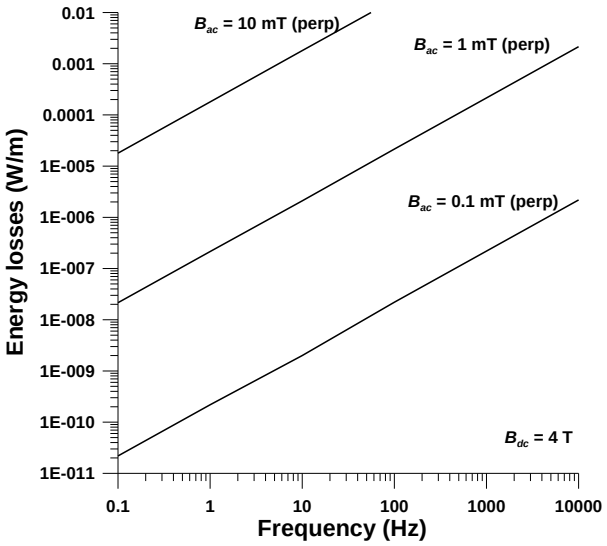

Fig. 5: Modelled losses as function of frequency for 0.1, 1 and 10 mT AC magnetic field ripple in a background DC field of 4 T.

4 Discussion

The AC losses need to be considered in the design phase of superconducting coils to be operated in the presence of an AC ripple field. In many cases the magnitude of the ripple field is controllable with protection measures, both in the current source (and its circuit) and by electromagnetic shielding of the coil from AC fields originating in external sources. In the absence of experimental data (at least for MgB_2 conductors) in the above 1 T measurement region, a simplified approach like the one presented here can give valuable guidelines for the electrical and thermal design of coils and their shielding systems. It establishes the order of magnitude and can point at critical fields, field orientations and frequencies.

From the modelled results the worst case for the conductor appears when the DC field is the highest, the ripple field is the highest, and the field orientation is perpendicular to the wide side of the conductor (particularly in a conductor with high aspect ratio). Unfortunately, these situations to a large extent occur simultaneously at the inner part of the coil. Any current ripple on the DC current in the coil results in a magnetic field ripple proportional to the DC field, which is highest at the inner part of the coil. Furthermore, at the coil ends, the field includes a substantial component perpendicular to the wide side of the tape.

When determining the acceptable magnetic field ripple level there are two main concerns. One is the total losses in the coil adding to the thermal load of the cooling machine. Obviously, the losses need to be kept low to lower the total power and cost of the cooling system. A second issue is the ability of the coil to withdraw locally generated heat. As seen in Fig. 3, a small increase in magnetic field ripple leads to a large increase in losses (cubic dependency), and a field orientation perpendicular to the wide side of the conductor leads to ten times higher losses than a parallel field. Hence, the majority of the losses may be dissipated within a relatively small volume. Consequently, the local heating may be severe in exposed parts of a coil.

The present work only deals with the hysteresis losses. In a real wire there are also other loss contributions which may be of importance, like eddy currents in the metal matrix, and flux-creep and flux-flow losses under DC operation, particularly close to the critical current. The latter can be of a significant magnitude if the conductor has a low *n*-value (the DC electric field along the conductor

being proportional to the *n*:th power of the current) [28]. For comparison, for a good MgB_2 conductor which typically has an *n*-value of 20, operates at 66% of I_c (using the standard 1 µV/cm criterion), and operates at a current of 100 A, the flux flow losses become $6 \cdot 10^{-6}$ W/m, comparable to the hysteresis loss values in Figs. 3-5.

Finally, we propose a very first overall estimate of tolerable AC ripple fields. In a 10 MW, 32 pole generator, such a coil may consist of 15 km of tape [5]. To keep the contribution from hysteresis losses below 0.5% of the total losses of a 10 MW wind turbine generator, no more than 1.5 W of losses can be tolerated in one race-track coil (when considering a cooling penalty factor at 20 K of 1000). The average losses should then be below approximately 10^{-4} W/m. Consider again Fig. 3, which shows losses per cycle. At 1 Hz, and the worst case, perpendicular AC ripple and 4 T DC background field, 10^{-4} W/m is reached at 7 mT. The corresponding number at 10 Hz is 4 mT and at 100 Hz 2 mT. Although varying with frequency, DC field and field orientation over the coil, these numbers give an estimate of an upper allowable limit for the ripple field. If the maximum DC magnetic field is 4 T, the ripple current should not be higher than approximately 0.1% of the DC current in the coil. Note that these considerations were based on the total hysteresis losses in the coil. Stricter criteria may be necessary due to local thermal properties, e.g. excessive heating in exposed parts of a coil.

5 Conclusions

We have reasoned towards a simplified treatment of the hysteresis losses due to ripple magnetic fields in MgB_2 conductors for wind turbine generator coils. With the method, the hysteresis losses, and thereby the tolerable magnetic field ripple can be estimated with the ripple magnitude and frequency, the in-field DC critical current and the geometry of the conductor as parameters. The method can be a valuable tool for designers of MgB_2 coils for generator field coils. First estimates of the tolerable losses indicate that the current ripple needs to be kept below approximately 0.1% of the DC current in the coil.

Acknowledgements

This work is part of the INNWIND.EU project supported by the FP7 framework of EU and the NOWITECH programme supported by the Research Council of Norway.

References

[1] M. Razeti, S. Angius, L. Bertora, D. Damiani, R. Marabotto, M. Modica, D. Nardelli, M. Perrella and M. Tassisto, Construction and Operation of Cryogen Free Magnets for Open MRI Systems, IEEE Trans. Appl. Supercond. 18 (2008) 882-886
[2] X.H. Li, X.J. Du, M. Qiu, Y.W. Ma and L.Y. Xiao, Design and experimental demonstration of an MgB_2 based 1.5 T MRI test magnet, Physica C 463-465 (2007) 1338-1341
[3] F. Sætre, I. Hiltunen, M. Runde, N. Magnusson, J. Järvelä, J. Bjerkli and E. Engebrethsen, Winding, cooling and initial testing of a 10 H superconducting MgB_2 coil for an induction heater, Supercond. Sci. Techn. 24 (2011) 035010
[4] S. Apiñániz, T. Arlaban, R. Manzanas, M. Tropeano, R. Funke, P. Kováč, Y. Yang, H. Neuman, X. Duluc and S. Sanz, Superconducting light generator for large offshore wind turbines, Presented at EUCAS2013, 15-19 September, Genova, Italy (2013) Paper No. 2M-LS-O5

[5] A.B. Abrahamsen, N. Magnusson, B.B. Jensen, D. Liu and H. Polinder, Design of an MgB_2 race track coil for a wind generator pole demonstration, Presented at EUCAS2013, 15-19 September, Genova, Italy (2013) Paper No. 3P-LS2-07
[6] E.A. Young, M. Bianchetti, G. Grasso, Y. Yang, Characteristics of AC loss in multifilamentary MgB_2 tapes, IEEE Trans. Appl. Supercond. 17 (2007) 2945–2948
[7] J. Kováč, J. Šouc, and P. Kováč, Experimental study of the AC magnetization loss in MgB_2 superconducting wires at different temperature, Physica C, 475 (2012) 1–4
[8] J Kováč, J. Šouc, P. Kováč, I. Hušek and F. Gömöry, Experimental study of magnetization AC loss in MgB_2 wires and cables with non-magnetic sheath, Physica C 495 (2013) 182-186
[9] H. Taxt, N. Magnusson and M. Runde, Apparatus for Calorimetric Measurements of Losses in MgB_2 Superconductors Exposed to Alternating Currents and External Magnetic Fields, Cryogenics 54 (2013) 44-49
[10] R. Fair, Final Scientific Report: Superconductivity for Large Scale Wind Turbines, General Electric, Global Research, 30 April, 2012
[11] H. London, Alternating current losses in superconductors of the second kind, Phys. Lett. 6 (1963) 162-165
[12] C.P. Bean, Magnetization of High-Field Superconductors, Rev. Mod. Phys. 36 (1964) 31-39
[13] E. Brandt and M. Indenbom, Type-II-superconductor strip with current in a perpendicular magnetic field, Phys. Rev. B 48 (1993) 12893-12906
[14] W.J. Carr, AC loss from the combined action of transport current and applied field, IEEE Trans. Magn. 15 (1979) 240-243
[15] N. Magnusson and S. Hörnfeldt, Losses in HTS Carrying AC Transport Currents in AC External Magnetic Fields, IEEE Trans. Appl. Supercond. 9 (1999) 785-789
[16] N. Schönborg and S.P. Hörnfeldt, Losses in a high-temperature superconductor exposed to AC and DC transport currents and magnetic fields, IEEE Trans. Appl. Supercond. 11 (2001) 4086-4090
[17] P. Dolez, B. des Ligneris, M. Aubin, W. Zhu and J. Cave, Effect of Combining a DC Bias Current with an AC Transport Current on AC Losses in a High Temperature Superconductor, IEEE Trans. Appl. Supercond. 9 (1999) 1065-1068
[18] K.W. See, C D. Cook and S.X. Dou, Innovative Calorimetric AC Loss Measurement of HTSC for Power Applications, IEEE Trans. Appl. Supercond. 21 (2011) 3261-3264
[19] Y. Fukumoto, H. J. Wiesmann, M. Garber and M. Suenaga, Alternating current losses in mono- and multicored silver sheathed $(Bi,Pb)_2Sr_2Cu_3O_{10}$ tapes at T=27 K in direct current magnetic fields, J. Appl. Phys. 78 (1995) 4584-4590
[20] N. Magnusson and A. Wolfbrandt, AC losses in high-temperature superconducting tapes exposed to longitudinal magnetic fields, Cryogenics 41 (2001) 721-724
[21] J.J. Rabbers, B. ten Haken, O.A. Shevchenko, H.H.J. ten Hate, Total ac loss of BSCCO/Ag tape in different orientations of the external magnetic field. Inst. Phys. Conf. Ser. (2000) 859-862
[22] A. Wolfbrandt, N. Magnusson and S. Hörnfeldt, AC Losses in a BSCCO/Ag Tape Carrying AC Transport Currents in AC Magnetic Fields Applied in Different Orientations, IEEE Trans. Appl. Supercond. 11 (2001) 4123-4127
[23] G.M. Zhang, L.Z. Lin, L.Y. Xiao and Y.J. Yu, The angular dependence of AC losses in BSCCO/Ag tapes under AC magnetic fields and AC transport currents, Cryogenics 43 (2003) 25–29
[24] B. ten Haken, J.J Rabbers and H.H.J. ten Kate, Magnetization and AC loss in a superconductor with an elliptical cross-section and arbitrary aspect ratio, Physica C 377 (2002) 156–164
[25] M. Ciszek, A.M. Campbell, S.P. Ashworth and B.A. Glowacki, Energy dissipation in high temperature ceramic superconductors, Applied Supercond. 3 (1995) 509-520
[26] H. Taxt, N. Magnusson, M. Runde and S. Brisigotti, AC Loss Measurements on Multi-filamentary MgB_2 Wires with Non-magnetic Sheath Materials, IEEE Trans. Appl. Supercond. 23 (2013) 8200204
[27] E. Pardo, Modelling of AC loss in coils made of thin tapes under DC bias current, IEEE Trans. Appl. Supercond. (2013) 10.1109/TASC.2013.2282495

[28] S. Mine, M. Xu, S. Buresh, W. Stautner, C. Immer, E.T. Laskaris, K. Amm and G. Grasso, Second Test Coil for the Development of a Compact 3 T MgB_2 Magnet, IEEE Trans. Appl. Supercond. 23 (2013) 4601404